Glucose Sensor Dynamics and the Artificial Pancreas

THE IMPACT OF LAG ON SENSOR MEASUREMENT AND CONTROLLER PERFORMANCE

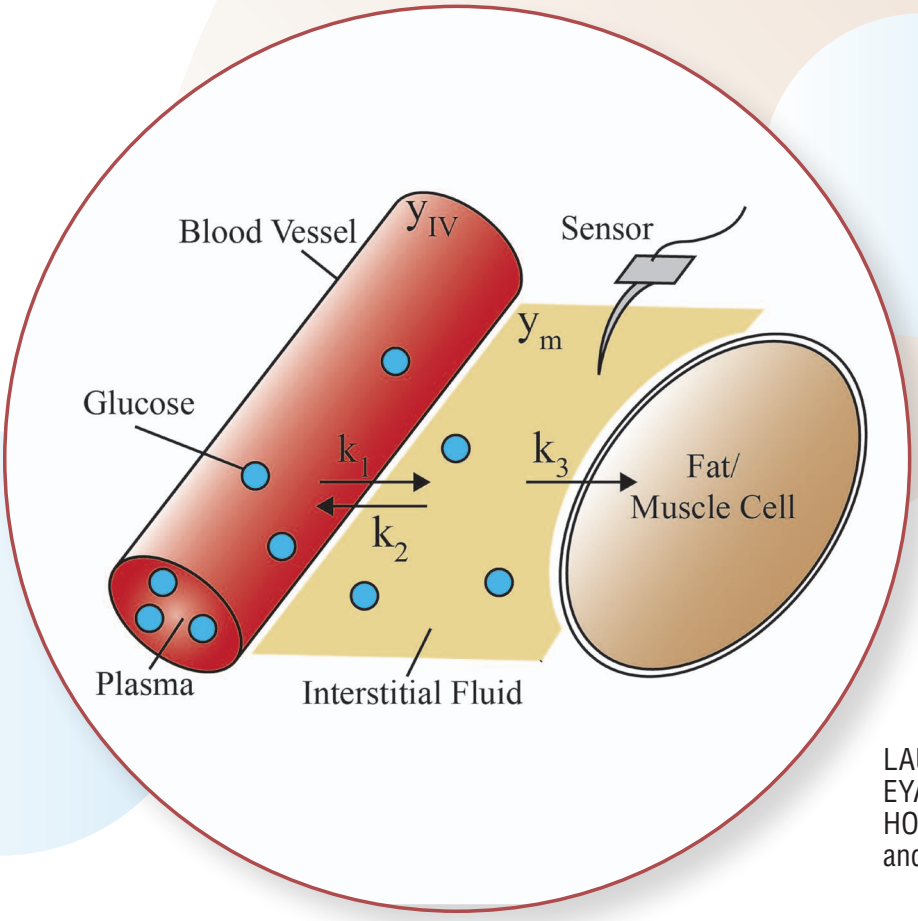

LAUREN M. HUYETT,
EYAL DASSAU,
HOWARD C. ZISSER,
and FRANCIS J. DOYLE III

Type 1 diabetes mellitus (T1DM) is a metabolic disorder characterized by the destruction of the pancreatic beta cells. With this disease, the body is no longer able to produce insulin, leading to chronically high concentrations of glucose in the blood (hyperglycemia) [1]. People with T1DM manage the disease by administering exogenous insulin doses as determined by multiple daily measurements of the blood glucose (BG) concentration; however, this approach requires significant effort from the patient and often achieves suboptimal results, leading to short- and long-term health complications [2]–[5].

The artificial pancreas (AP), a device intended to provide automated treatment for T1DM, has been under development for several decades [6]–[9] (refer to [10] for a full review). The AP comprises a control algorithm, an insulin pump, and a glucose concentration sensor. The system is

Digital Object Identifier 10.1109/MCS.2017.2766322
Date of publication: 19 January 2018

depicted in Figure 1. The control algorithm delivers insulin to maintain the BG within the clinically desired range. This range is generally taken as 70–180 mg/dL, with the 2017 American Diabetes Association Standards of Medical Care recommending a preprandial BG of 80–130 mg/dL and a peak postprandial BG <180 mg/dL [10]–[12].

The performance of the AP is constrained by the physical limitations introduced by the insulin pump and glucose sensor. Most clinically tested AP devices have used subcutaneous (SC) insulin delivery and glucose sensing devices, which are minimally invasive and commercially available for use [10], [13]. However, the SC route introduces transport processes in both the absorption of insulin from the SC space to the blood and the diffusion of glucose from the blood to the SC space, adding time lags to the control loop [10], [14], [15].

To improve the performance of the AP, researchers have incorporated methods to compensate for these lags through the design of the control algorithm, as in [16]–[18], and in the sensor signal processing algorithms, as in [19] and [20]. Additionally, many AP systems undergoing clinical testing are not fully automated; instead, they require the user to manually announce the onset of a meal, after which the controller issues a preemptive insulin bolus. Several strategies for meal announcement have been tested (see [21] for a detailed discussion of this topic). Such hybrid systems have been recently evaluated in clinical studies using model predictive control, proportional-integral-derivative (PID) control, and fuzzy logic control schemes. These AP designs have been able to achieve an average of 68–81% of time in the range 70–180 mg/dL, depending on the protocol, length of closed loop, degree of supervision, and controller design [22]–[27].

To make further improvements in the performance of the AP, it may be necessary to alter the system components, thereby changing the dynamics of the open-loop process. There are means to reduce the lags observed with the SC route, such as implanting the pump and/or sensor in the intraperitoneal (IP) space. This location is closer to major vasculature, which increases the speed of glucose diffusion and insulin absorption as compared to that observed in the SC space. Insulin delivery through the IP route has been shown to reduce the frequency of hypoglycemic episodes and improve the glycemic control of people with T1DM [28]–[30]. However, the benefit of this placement must outweigh the cost of increased invasiveness [31], [32]. Devices in the IP space require surgery for placement, while SC devices are primarily external and involve only a small transcutaneous insertion that can be done by the patient.

The improvement in AP performance gained by decreasing the insulin pharmacokinetic time constant was presented in a previous study [33]. Additionally, improved controller performance has been observed in clinical studies using IP or inhaled insulin, which are both associated with faster pharmacokinetic and pharmacodynamic properties than the SC space [34]–[36]. In this article, a complementary study to [33] is performed to quantify the impact that glucose sensing lag has on an AP that uses either SC or IP insulin delivery [37]. As discussed in "Summary," first the glucose measurement process is modeled and the effects of the sensor lag on the measurement accuracy are explored. The impact of sensor lag on the performance of an AP controller is then investigated through frequency response analysis and simulation studies.

CONTINUOUS GLUCOSE SENSING

Modeling the Sensor Response

Commercially available continuous glucose sensors measure the glucose concentration in the interstitial fluid (ISF), rather than the blood. For details, see "What Do Glucose Sensors Measure?" The diffusion process between the blood and the ISF means that the concentration measured by the glucose sensor may lag behind the BG, especially when the BG is increasing or decreasing at a high rate of change. To quantify this lag, a two-compartment model can be used to represent the glucose diffusion process.

Figure S1 demonstrates the two-compartment system. The first compartment is the blood within the blood vessel, and the second is the ISF. Glucose diffuses between the blood vessel and the ISF and vice versa. Glucose is also taken up from the ISF into cells. A mass balance can be conducted on the ISF compartment to determine how the concentration in that compartment evolves over time. The resulting first-order model for ISF glucose concentration as a function of the glucose concentration in the major blood vessels is given by

$$\frac{dy_m(t)}{dt} = -(k_3 + k_2)y_m(t) + k_1 \frac{V_b}{V_{isf}} y_{IV}(t), \tag{1}$$

where $y_m(t)$ is the glucose concentration measured by the sensor (mg/dL); $y_{IV}(t)$ is the glucose concentration in the blood (mg/dL); k_1, k_2, and k_3 are the rate constants for the diffusion processes as defined in Figure S1; and V_b and V_{isf} are the volumes of the blood and ISF, respectively. With both $y_m(t)$ and $y_{IV}(t)$ expressed as the deviation from the steady-state value, this equation can be expressed as a transfer function in the Laplace domain

$$G_S(s) = \frac{Y_m(s)}{Y_{IV}(s)} = \frac{K}{\tau_S s + 1}. \tag{2}$$

The identifiable parameters in this transfer function model are the sensor time constant $\tau_S = 1/(k_3 + k_2)$ (min) and the model gain $K = k_1 V_b / ((k_3 + k_2) V_{isf})$. The model gain K is assumed to be one when the sensor is properly calibrated, since the sensor measurement is expected to equal the BG measurement at steady state.

Since the most challenging aspects of AP design involve time periods where the BG is changing rapidly (after meals or

Summary

The AP has the potential to improve health outcomes for people with T1D. Most AP designs use commercially available insulin pumps and glucose sensors that operate in the SC space; however, the absorption of insulin from the SC space to the blood and the diffusion of glucose from the blood to the SC space introduce lags to the control loop. This lag may be reduced through alternative device placement, such as in the IP space, but the increased invasiveness of this approach must be justified by the resulting improvements in control. Previous studies have demonstrated the improvements in AP performance gained through faster insulin action. This article provides a framework to explore the return on investment gained by reducing the glucose sensor diffusion lag, using methods from control theory in combination with simulation studies. A range of potential sensor lags are evaluated for an AP with a model-based PID controller using either IP or SC insulin delivery. The approach presented here could be used to develop both sensor technologies and AP algorithms to evaluate the tradeoffs between sensor lag and clinical outcome.

during exercise), the filtering effect of the sensor dynamics is expected to have a detrimental impact on the control quality. This effect is demonstrated in the Bode plot in Figure 2. The smaller the sensor lag is, the higher frequencies of input can be tolerated without losing response tracking.

An assessment of sensor technology in 2009 found that the overall physiological lag was 3–12 min, with the intrinsic electrochemical sensor lag no more than 1–2 min [38]. Data from a human clinical study showed that SC sensors have time constants ranging from 2 to 20 min [39]. Lastly, the results of a tracer kinetics study showed that the time constant in the SC space for people with T1DM was 11.0 ± 3.3 min [40].

Placing the sensing mechanism in a more highly vascularized area, such as the IP space, has been shown to facilitate more rapid sensing of glucose changes. The experimental data presented in [31] were used to quantify the dynamic response of glucose sensors placed in either the SC or the IP space of nondiabetic swine. This animal model is often used for studies that require a model of the human endocrine system. The data showed that the sensors implanted in the IP space of swine had faster dynamics than the SC sensors placed in the same animal. The distribution of fitted time constants of the model in (2) for sensors in each space was 5.6 ± 2.9 min for the IP sensors and 12.4 ± 3.6 min for the SC sensors [31]. In general, the IP sensors had a lower mean time constant and a tighter distribution, while the SC sensors had a higher mean time constant and wider distribution.

In the present computational work, τ_S is varied to investigate a wide range of sensor dynamics (0–30 min) using the model in (2), with $K = 1$. The intent is not to replicate a specific sensor placement but to interrogate the relationship between sensor lag and AP performance. This range of values was chosen to capture sensor lags that may be encountered with the commonly used SC electrochemical glucose sensors as well as emerging technologies in sensor development that seek to improve other aspects of the sensor, such as lifetime, convenience, accuracy, or usability [41]–[44]. An ideal BG sensor is represented by the case when $\tau_S = 0$ min.

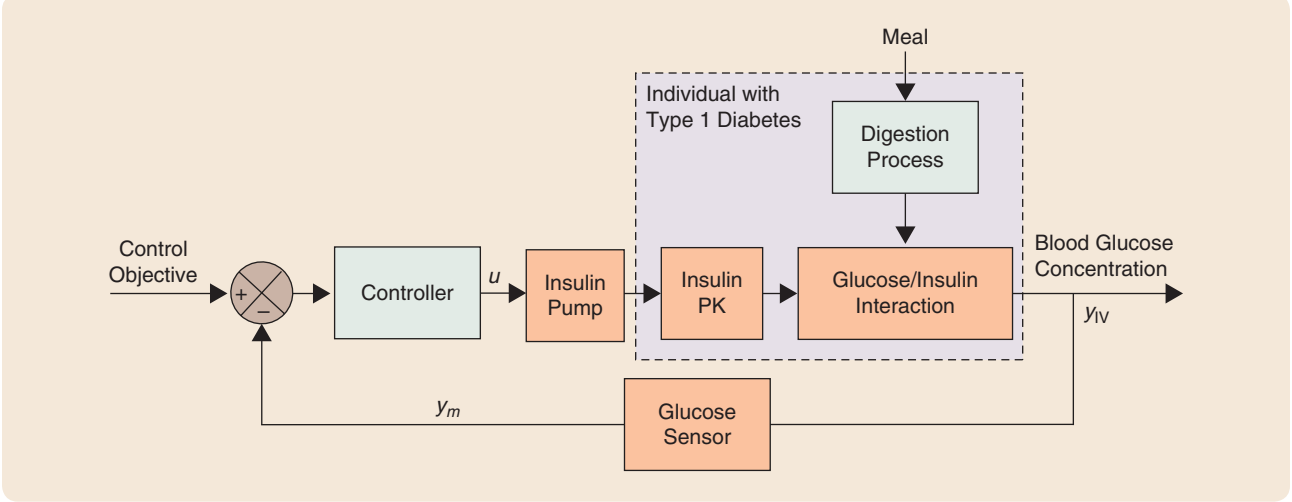

FIGURE 1 A block diagram representation of the artificial pancreas. The controller receives the measured glucose concentration, y_m, and compares it to the control objective. The controller then determines the desired insulin dose u and sends it to the insulin pump. Depending on the insulin delivery route, the insulin is absorbed into the bloodstream with a specific pharmacokinetic (PK) profile. The insulin then acts to change the glucose concentration, which is affected by disturbances such as meals. The blood glucose concentration is measured by the sensor. Depending on the sensor type and placement, the sensor measurement may experience a dynamic lag. The shaded blocks show the parts of the process that can be changed through pump and sensor site selection.

What Do Glucose Sensors Measure?

Glucose enters the body through the ingestion of food. After the glucose is absorbed through digestion, it travels through the major and minor blood vessels to reach the brain, muscle cells, and other tissues. To reach individual cells, the glucose first diffuses from capillaries into the ISF, as depicted in Figure S1. The ISF of the SC space has been established as a minimally invasive site for a sensor to provide a continuous estimation of the BG concentration. Commercially available glucose sensors detect the glucose once it has reached the ISF using a transcutaneous electrode or other sensing mechanism [64]. The signal from this sensor must be calibrated to the BG by taking a capillary blood measurement with a handheld meter.

While the sensor measures the glucose concentration in the ISF, the raw sensor signal is calibrated using a measurement of the concentration in the capillary blood. The gradient between the absolute glucose concentration in the blood and the ISF at steady state has been reported as anywhere from 50 to 100%, but is difficult to establish definitively due to the lack of techniques for directly measuring the concentration of glucose in the ISF [40], [65]. However, many studies have established the accuracy of SC glucose sensors that are calibrated to BG values across a wide range of physiological BG values, making it a reasonable assumption that the concentrations are directly proportional or equal at steady state [66]–[68]. Regardless of the true gradient, the sensor reading in mg/dL will be equal to the BG in mg/dL at steady state if the sensor is properly calibrated.

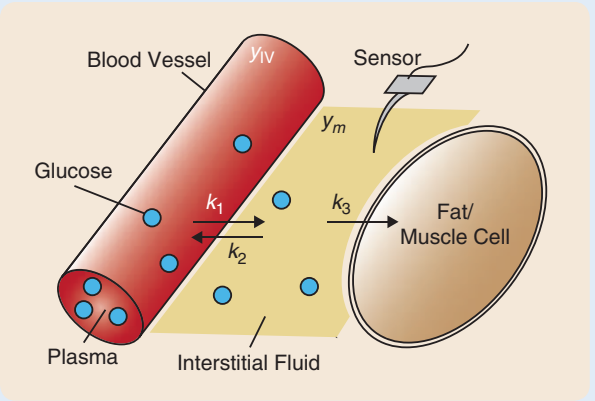

FIGURE S1 A schematic representation of the glucose transport process. First, the glucose diffuses from the blood vessel to the interstitial fluid. The sensing element is placed within the interstitial fluid and detects the glucose concentration there. The glucose is absorbed from the interstitial fluid into the surrounding fat and muscle cells to be used for energy. This diagram is based on the model presented in [65].

Impact of Lag on Sensor Accuracy

A dynamic lag in the measurement process leads to error between the true and measured BG values. One measure of this error is determined by the sensor response to a ramp input [45]. The ramp must be selected to have the maximum rate of change that is expected for the process. For a ramp of slope a, the upper bound on the error is given by

$$\epsilon_{\max} = \left| y_m(t) - y_{IV}(t) \right|_{\max}, \tag{3}$$

where $y_{IV}(t) = \alpha t$ (a ramp input in BG concentration). The time-domain response to a ramp for a transfer function with first-order dynamics and unity gain, such as that in (2), is determined by substituting the Laplace transform of the ramp $(Y_{IV}(s) = \alpha/s^2)$ into (2) and taking the inverse Laplace transform to obtain

$$y_m(t) = \alpha\tau_S(e^{-t/\tau_S} - 1) + \alpha t. \tag{4}$$

By substituting (4) into (3), the error reduces to

$$\epsilon_{\max} = \left| \alpha\tau_S(e^{-t/\tau_S} - 1) \right|_{\max}. \tag{5}$$

The maximum error occurs when $t \gg \tau_S$, giving

$$\epsilon_{\max} = \left| a\tau_S \right|. \tag{6}$$

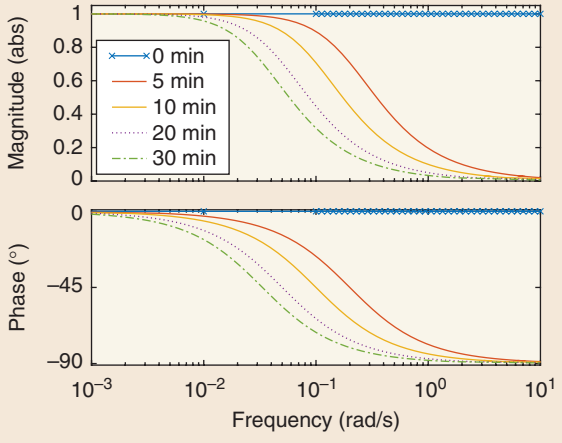

FIGURE 2 A Bode plot showing the deterioration of sensor response for values of τ_S from 5 to 30 min. The smaller the sensor lag is, the higher frequencies of input can be tolerated without losing response tracking.

The maximum rate of change expected in glucose concentration data can be estimated as between an absolute value of 4 and 5 mg/dL/min, as seen in clinical data [46], [47]. The upper bounds on the measurement error given a ramp of 4 and 5 mg/dL/min for sensor time constants ranging

from 5 to 30 min are shown in Table 1. Reducing the glucose sensor lag will reduce the upper bound on the dynamic measurement error in a linear relationship.

The upper bound on the error provided by (6) is a conservative estimate for BG monitoring applications, where the rate of change is unlikely to continue at the maximum value for times $t \gg \tau_S$. Therefore, it is useful to consider the transient error response to a ramp of maximum slope lasting 15 min. Figure 3 shows the transient response for simulated glucose sensors with τ_S equal to 5, 10, 20, and 30 min for a BG ramp of slope −4.5 mg/dL/min. The starting glucose concentration is set to 130 mg/dL. After 15 min, the BG has crossed the threshold into hypoglycemia; however, none of the simulated sensors would have detected this safety risk at the time it happened. The timely detection of rapid changes in BG is critical to the safe and effective operation of the AP, especially if the change presents an immediate health risk such as hypoglycemia. Figure 3 demonstrates the danger of a lagging sensor measurement, which produces an error that is correlated in time and becomes larger for higher rates of change.

The measurement error due to dynamic sensor lag that would occur for typical BG trajectories was investigated using retrospective analysis of data from a previous clinical study. During a 24-h clinical evaluation of an AP device in 12 subjects, BG measurements were taken every 30 min or every 15 min during exercise and hypo- or hyperglycemic episodes [48]. The BG measurements were taken from venous blood using a YSI 2300 STAT Plus glucose and lactate analyzer (Yellow Springs Instruments, Yellow Springs, Ohio), which is considered to be the gold standard in glucose measurement. Using this data and the sensor model in (2), measurements from sensors with different time constants were simulated. An example of the experimental YSI measurements and simulated sensor measurements for one subject are shown in Figure 4.

A histogram of the resulting pointwise error between BG measurement and simulated sensor measurement for the 12 subjects combined is shown in Figure 5. The error was also analyzed using the mean absolute relative difference (MARD) and the Clarke error grid, which are two frequently used methods to quantify glucose sensor error. For details on these methods, see "Measures of Glucose Sensor

TABLE 1 A summary of dynamic error characteristics resulting from simulated glucose sensors with different values of τ_S.

	τ_S (min)			
	5	**10**	**20**	**30**
ϵ_{max} (mg/dL)				
a = 4 mg/dL/min	20	40	80	120
a = 5 mg/dL/min	25	50	100	150
MARD (%)	1.9	3.6	6.4	8.6
Clarke zone (%)				
A	98.9	98.4	95.5	90.1
B	1.1	1.6	4.5	9.7
C	0	0	0	0
D	0	0	0	0.16
E	0	0	0	0
A+B	100	100	100	99.8

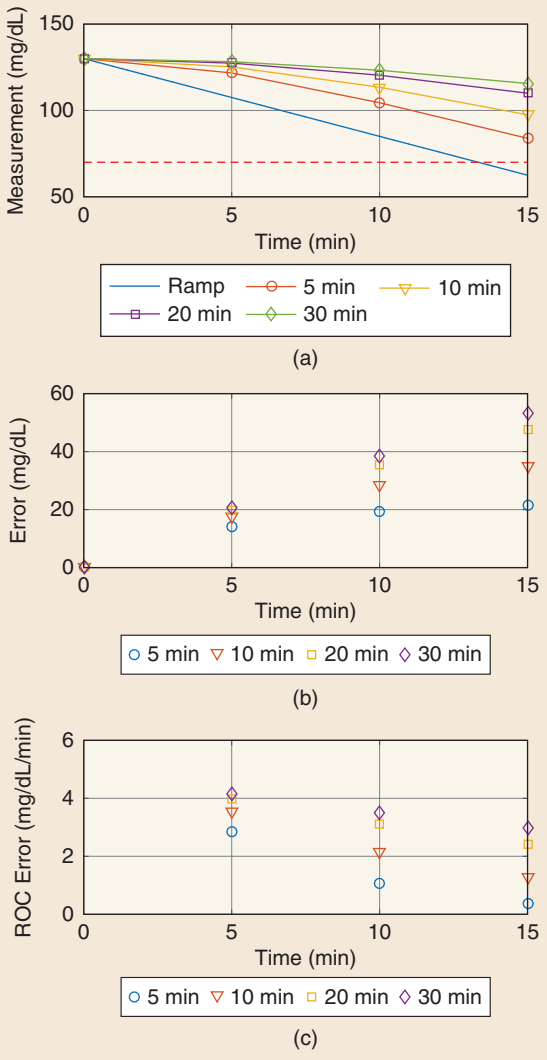

FIGURE 3 Error introduced by a sensor lag in the transient time response for a blood glucose concentration ramp with slope −4.5 mg/dL/min. The red dashed line shows the hypoglycemia threshold of 70 mg/dL/min. The varying values of τ_S are represented by symbol type and color. The symbols indicate the sampling time of a glucose sensor, which is 5 min. (a) The ramp blood glucose concentration and simulated sensor measurements over time. (b) The error between the blood glucose concentration ramp and the simulated sensor measurements. (c) The error between the rate of change (ROC) estimated from the sensor versus the ROC of the blood glucose concentration.

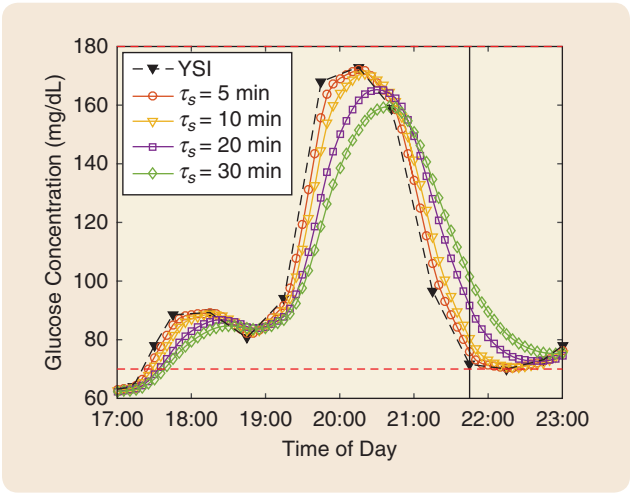

FIGURE 4 Blood glucose measurement data (YSI) from a clinical trial of an artificial pancreas. Simulated sensor measurements with different dynamic lags are distinguished by symbol. The vertical black line can be used to visualize the offset between the blood glucose concentration measurement and the sensor measurement at a given instant in time during a decrease toward hypoglycemia.

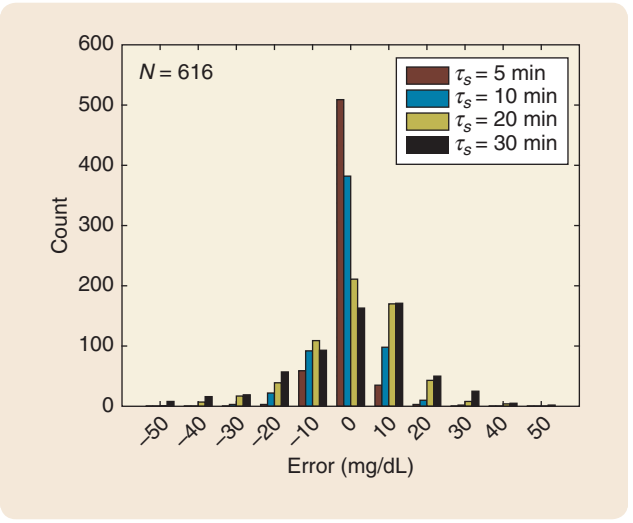

FIGURE 5 A histogram of the error induced by dynamic sensor lag for simulated sensor measurements based on clinical blood glucose concentration data. The error is defined as the reference blood glucose measurement subtracted from the simulated sensor measurement. The total number of reference-sensor data pairs is 616.

Error." The MARD for each simulated sensor run on the clinical data is shown in Table 1. As seen in the table, the MARD ranges from 1.9 to 8.6% for a τ_S of 5–30 min. Additionally, as shown in Figure 6 and Table 1, 100% of points fell within the A (accurate) or B (benign error) zones of the Clarke error grid for values of τ_S from 5 to 20 min and 99.8% of points for a τ_S of 30 min.

The results of the MARD and the Clarke error grid analyses show that the pointwise error caused by the sensor lag alone does not exceed limits for clinical usability. However, the dynamic nature of the error is expected to cause problems for the AP, which relies on the glucose trajectory over time to make accurate and timely insulin dose recommendations. A lag in the measurement will lead to a lag in the

Measures of Glucose Sensor Error

The performance of continuous glucose monitors can be evaluated by examining the error between measurements taken by a continuous glucose monitor and measurements taken using a gold standard reference method at the same time points. The most commonly used reference method is venous blood using a YSI 2300 STAT Plus glucose and lactate analyzer. A frequently reported error measure is the MARD, which is typically used to provide a single number that characterizes glucose sensor error during a given time period. This measure is calculated as

$$\text{MARD} = \frac{1}{n}\sum_{i=1}^{n}\frac{|y_{m,i} - y_{IV,i}|}{y_{IV,i}} \times 100, \tag{S1}$$

where $y_{m,i}$ is the glucose sensor measurement and $y_{IV,i}$ is the reference BG measurement at the same time point [64]. The MARD is considered an important value when reporting glucose sensor accuracy and may determine whether the glucose sensor can be used as a replacement for capillary blood measurements to determine insulin dosing. For example, it is stated in [66] that glucose sensors must reach a MARD below 10% before they can be approved for use in determining insulin dosage.

While the MARD gives a general idea of the glucose sensor performance, it does not demonstrate how that error might affect T1DM treatment decisions. For this reason, the Clarke error grid was developed to determine the clinical implications of the error [69]. In this method, glucose sensor measurements are plotted versus gold standard reference measurements of the BG taken at the same time point on a graph that is divided into five zones, as shown in Figure 6. The zones are 1) A, where the glucose sensor measurement is within 20% of the reference; 2) B, where the error is greater than 20% of the reference, but the treatment determined from the glucose sensor and reference would have been the same; 3) C, where unnecessary treatment would be given that could lead to dangerous hyperglycemia or hypoglycemia; 4) D, where dangerous hyperglycemia or hypoglycemia would go undetected; and 5) E, where the treatment given would be the opposite of the required treatment [69]. According to one source, the percentage of points in the A and B zones should be higher than 98% to be acceptable [64].

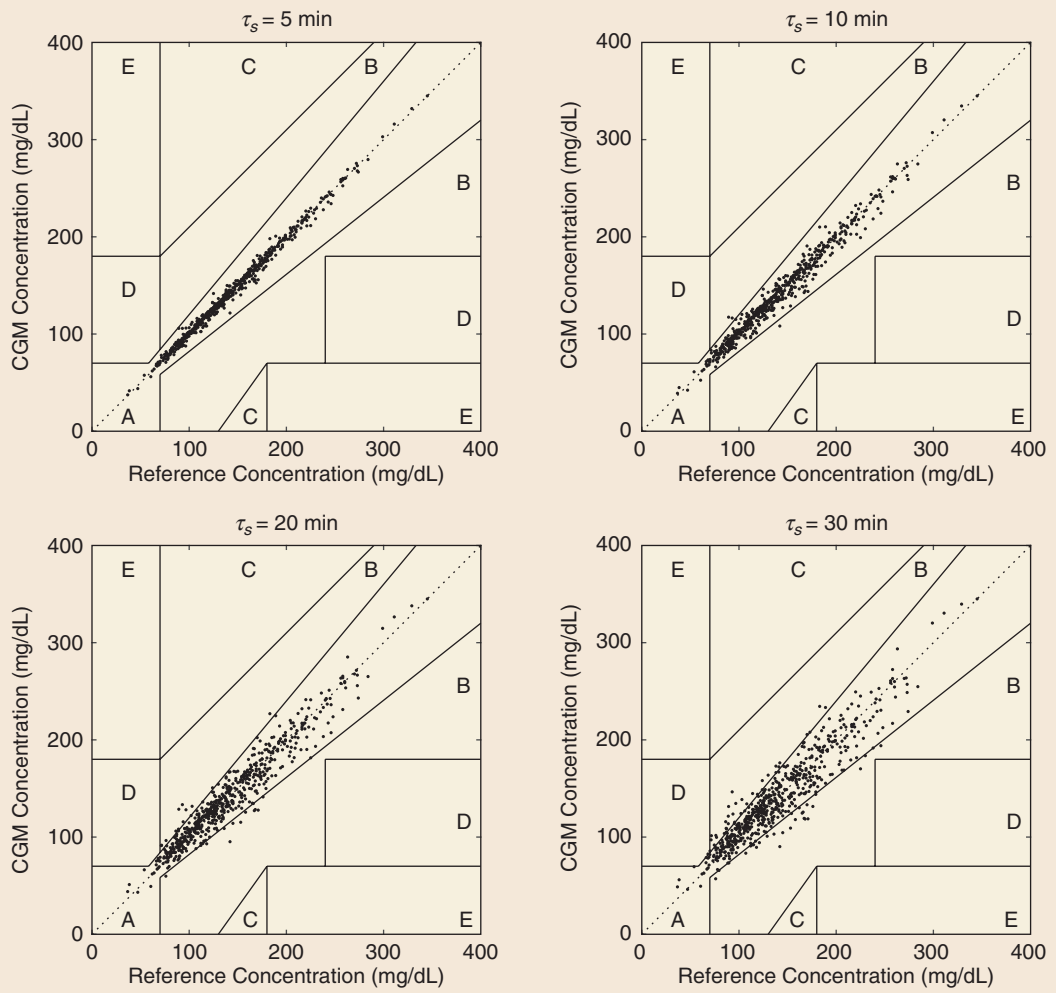

FIGURE 6 A Clarke error grid for simulated sensors with different time constants. The Clarke error grid is used to demonstrate the clinical implications of a sensor error [continuous glucose monitor (CGM)]. The grid shows that for values of τ_S from 5 to 20 min, all of the points fall into the A+B (acceptable error) zones. For τ_S equal to 30 min, 99.8% of points fall into the acceptable error zones, with 0.16% in the D zone. The total number of points is 616.

controller action, especially when responding to large disturbances such as meals. In the following sections, control theory and simulation studies are used to quantify the effect of sensor lag on an AP controller.

EFFECTS OF SENSING LAG ON CONTROLLER PERFORMANCE

Controller Design and Tuning

Following an analogous approach to the one outlined in [33], a model-based PID controller was designed and used to interrogate the effects of sensor dynamics on controller performance. The following third-order discrete-time model of insulin action on BG has been previously identified, with different parameters to represent either IP or SC insulin delivery [49], [50]

$$M_D = \frac{K(\mathrm{TDI})^{-1} z^{-3}}{(1-a_1 z^{-1})(1-a_2 z^{-1})^2}, \tag{7}$$

where TDI (U) is the total daily insulin dose of the patient and the sampling time is 5 min. The inclusion of the total daily dose allows the gain to be personalized based on each patient's response to insulin. The model parameters are given in Table 2, based on previous work [49]–[50]. The model was converted to continuous time using the zero-pole matching method [52] to obtain the following third-order continuous model:

$$M_C = \frac{K'(\mathrm{TDI})^{-1}}{(\tau_1 s+1)(\tau_2 s+1)^2}. \tag{8}$$

The parameters for the resulting continuous model are also shown in Table 2. The third-order model was then

reduced to a second-order model using Skogestad's half rule [53] to obtain

$$G = \frac{K'(\text{TDI})^{-1}e^{-\hat{\theta}s}}{(\hat{\tau}_1 s+1)(\hat{\tau}_2 s+1)}, \tag{9}$$

where the reduced-order model parameters are determined by the relations

$$\hat{\tau}_1 = \tau_1, \quad \hat{\tau}_2 = \tau_2 + \frac{\tau_2}{2}, \quad \text{and} \quad \hat{\theta} = \frac{\tau_2}{2} + \frac{\Delta t}{2}, \tag{10}$$

with the resulting reduced model parameters included in Table 2. Here, Δt is the sampling time that will be used in the implementation of the controller. Note that the transfer function in (9) describes the change in glucose concentration (mg/dL) for a change in insulin delivery (U/h).

The controller parameters were determined using the model in (9) with internal model control tuning rules. For more details on this method, see "Internal Model Control Tuning for PID Controllers." The choices for τ_C in this study were determined from the dominant time constants (τ_{dom}) of the IP and SC models, which were found by inspection of the step response to be 285 and 564 min for the IP and SC systems, respectively. Values for τ_C were selected as $\tau_{\text{dom}}[0.1, 0.3, 0.5, 0.7]$ as indicated by the tuning guidelines in [45]. The PID controller was then implemented using the discrete position form with a sampling time of 5 min

$$u(k) = \bar{u} + K_C\left[e(k) + \frac{\Delta t}{\tau_I}\sum_{j=1}^{k} e(j) + \frac{\tau_D}{\Delta t}[e(k) - e(k-1)]\right], \tag{11}$$

where $u(k)$ is the insulin delivery computed by the controller (U/h), $\bar{u}$ is the steady-state insulin delivery rate (U/h), K_C is the controller gain ([U/h]/[mg/dL]), τ_I is the integral time constant (min), τ_D is the derivative time constant (min), and $e(k)$ is the difference between the glucose measurement and the setpoint of 110 mg/dL. While there is no obvious choice for setpoint based on physiology, 110 mg/dL was chosen because it is in the middle of the tight glycemic control range of 80–140 mg/dL. This setpoint has been used in previous AP designs, including in [33].

Frequency Response and Robustness Analysis

For the AP to be safe for clinical use, it must be robust to model uncertainty. The human body's reaction to insulin can vary depending on the time of day, hormonal changes, exercise, and other factors that are part of daily life. Changes in insulin sensitivity of up to 50% have been experimentally observed [54]. These changes can be considered as perturbations to the gain and delay of the nominal model. A controller is said to be robust if it is insensitive to differences between the actual system being controlled and the model of the system that was used determine the controller tuning parameters. Robustness is determined by checking that the system is stable and meets performance requirements even for the worst-case scenario of model uncertainty [55]. A robust design is crucial for AP applications since the controller will be part of a medical device that needs to meet its design specifications even in the face of model uncertainty introduced between different patients or over time in the same patient.

In this article, two methods were used to analyze the impact of glucose sensing lag on the robustness of the AP system: 1) gain and phase margin analysis and 2) robust stability and performance analysis. See "Methods for Determining Robustness" for details on these methods.

TABLE 2 Parameters for the discrete, continuous, and reduced models of intraperitoneal (IP) and subcutaneous (SC) insulin action [37].

	Discrete			Continuous		
	K (h · mg/dL)	a_1	a_2	K' (h · mg/dL)	τ_1 (min)	τ_2 (min)
IP	–15	0.98	0.75	–12,000	247	17
SC	–0.30	0.98	0.965	–12,294	247	140

	Reduced		
	$\hat{\tau}_1$ (min)	$\hat{\tau}_2$ (min)	$\hat{\theta}$ (min)
IP	247	26	11
SC	247	210	73

Internal Model Control Tuning for PID Controllers

Internal model control is a model-based controller design method developed to give an analytical expression for a controller based on a dynamic model of the process [45]. The design procedure leaves a single tuning knob, the characteristic time constant τ_c, which sets the robustness of the controller. Internal model control design for a second-order transfer function model yields an equivalent PID controller, so direct relations between the model parameters and the PID tuning parameters can be expressed [45]. For the second-order transfer function model with time delay

$$G = \frac{\hat{K}e^{-\hat{\theta}s}}{(\hat{\tau}_1 s+1)(\hat{\tau}_2 s+1)}, \tag{S2}$$

the tuning parameters for a PID controller can be calculated as given in [45] as

$$K_C = \frac{\hat{\tau}_1 + \hat{\tau}_2}{\hat{K}(\tau_C + \hat{\theta})}, \tag{S3}$$

$$\tau_I = \hat{\tau}_1 + \hat{\tau}_2, \tag{S4}$$

$$\tau_D = \frac{\hat{\tau}_1\hat{\tau}_2}{\hat{\tau}_1 + \hat{\tau}_2}. \tag{S5}$$

The human body's reaction to insulin can vary depending on the time of day, hormonal changes, exercise, and other factors that are part of daily life.

Gain and Phase Margin

The calculated gain and phase margins for varying values of τ_S and τ_C are shown in Tables 3 and 4. A Bode plot demonstrating the calculation of the gain and phase margin for IP insulin with $\tau_C = 0.1\tau_{\text{dom}}$ is shown in Figure 7. These values show that increasing τ_S and/or decreasing τ_C reduces the margin for error before instability is reached. Overall, the IP system has higher margins than the SC system, which is due to the faster actuation available through the IP route.

A general recommendation for the gain and phase margin given in [45] states that a well-tuned controller will have a gain margin between 1.7 and 4.0 and a phase margin between 30 and 45° [45]. The gain and phase margins obtained for the controller design presented in this article are similar to those presented in [33], in which the impact of insulin pharmacokinetic and pharmacodynamic properties on the AP was evaluated. As in that study, the gain and phase margins in Tables 3 and 4 are within or higher than the range of published

Methods for Determining System Robustness

Gain and phase margins can be used to perform a preliminary screening of the system robustness. These two measures are based on the frequency response analysis of the open-loop transfer function. The gain margin is calculated by $1/(AR_c)$, where AR_c is the magnitude at the critical frequency where the phase crosses –180°. The phase margin is calculated as $180 + \phi_g$, where ϕ_g is the phase at the gain-crossover frequency where the magnitude equals one [45]. The gain margin reflects how much the open-loop gain can increase before reaching instability, while the phase margin shows how much the open-loop delay can increase before instability occurs.

Robust stability and performance analysis is a more formal measure of system robustness to model uncertainty. As described in [55], the family of possible plants Π_I that exist given a nominal process model with specified uncertainty was represented using multiplicative uncertainty

$$\Pi_I:\ G_P(s) = G(s)(1 + w_I(s)\Delta_I(s)); \quad |\Delta_I(j\omega)| \le 1, \quad \text{for all } \omega, \tag{S6}$$

where G_P is a potential process model and G is the nominal process model. The uncertainty weight fulfills the relation $|w_I(j\omega)| \le I_I(\omega)$, for all ω where

$$I_I(\omega) = \max_{G_P \in \Pi_I} \left| \frac{G_P(j\omega) - G(j\omega)}{G(j\omega)} \right|. \tag{S7}$$

The condition for robust stability (RS) is then given by

$$\text{RS} \Leftrightarrow \ \|w_I T\|_\infty < 1, \quad \text{for all } \omega, \tag{S8}$$

where T is the complementary sensitivity function and w_I is the multiplicative uncertainty weight as defined previously. The weight for parametric uncertainty in the gain and delay for the model in (9), is given by

$$w_I = \frac{(1 + \frac{r_k}{2})\theta_{\max} s + r_k}{\frac{\theta_{\max}}{2} s + 1}, \tag{S9}$$

where $r_k = (K_{\max} - K_{\min})/(K_{\max} + K_{\min})$ and $\theta_{\max}$ is the maximum uncertainty in the delay considered [55]. In this study, gains on the range $K_{\text{nom}}[1 - \delta, 1 + \delta]$ were considered, where δ was allowed to vary from 0.1 to 0.9. The nominal gain K_{nom} was chosen as the nonpersonalized gain of –200 (mg/dL)/(U/h) [49]–[51]. The maximum delay uncertainty tested was 30 min.

The robust performance criterion is used to determine whether specified performance measures will be met in the presence of model uncertainty. The condition for robust performance (RP) is

$$\text{RP} \Leftrightarrow \max_{\omega}(|w_P S| + |w_I T|) < 1, \tag{S10}$$

where S is the sensitivity function. The performance weight w_P is given by

$$w_P(s) = \frac{\frac{s}{M} + \omega_B^*}{s + \omega_B^* A}, \tag{S11}$$

where M is the maximum peak of the sensitivity function, A is the steady-state tracking error, and ω_B^* is the bandwidth frequency [55]. In this study, $A = 10^{-2}, \omega_B^* = 5 \times 10^{-5}$ rad/s, and $M = 2$. The value of A was chosen to be approximately zero because it is important for the controller to track the setpoint closely at steady state, even in the presence of model uncertainty. The value for M was chosen in accordance with the recommendation in [45]. The bandwidth frequency was selected based on the bandwidth of a closed-loop system using SC insulin delivery, which is the current state-of-the-art configuration used in clinical evaluations [10].

TABLE 3 The gain margin for varying sensor time constants and tuning parameters [37].

Intraperitoneal Delivery

	τ_C			
τ_S	$0.1\tau_{dom}$	$0.3\tau_{dom}$	$0.5\tau_{dom}$	$0.7\tau_{dom}$
0 min	5.7	14	22	30
10 min	4.1	10	16	22
20 min	3.9	9.5	15	21
30 min	3.8	9.3	15	20

Subcutaneous Delivery

	τ_C			
τ_S	$0.1\tau_{dom}$	$0.3\tau_{dom}$	$0.5\tau_{dom}$	$0.7\tau_{dom}$
0 min	2.8	5.2	7.6	10
10 min	2.5	4.7	6.8	9.0
20 min	2.3	4.4	6.4	8.4
30 min	2.2	4.2	6.1	8.0

TABLE 4 The phase margin for varying sensor time constants and tuning parameters [37].

Intraperitoneal Delivery

	τ_C			
τ_S	$0.1\tau_{dom}$	$0.3\tau_{dom}$	$0.5\tau_{dom}$	$0.7\tau_{dom}$
0 min	74°	83°	86°	87°
10 min	61°	78°	82°	84°
20 min	51°	72°	79°	82°
30 min	44°	67°	75°	79°

Subcutaneous Delivery

	τ_C			
τ_S	$0.1\tau_{dom}$	$0.3\tau_{dom}$	$0.5\tau_{dom}$	$0.7\tau_{dom}$
0 min	58°	73°	78°	81°
10 min	53°	70°	77°	80°
20 min	49°	68°	75°	79°
30 min	46°	66°	73°	77°

guidelines in [45] due to the conservative controller design required for safety in medical applications. Smaller values of gain and phase margin can lead to an oscillatory response, which must absolutely be avoided in the AP system.

Robust Stability and Performance

The robust stability and performance analyses were conducted to determine how much model uncertainty in the gain and delay would be tolerated for a specified sensor time constant and controller tuning. Gains on the range $K_{nom}[1-\delta, 1+\delta]$ were considered, where δ was allowed to vary from 0.1 to 0.9. The nominal gain k_{nom} was chosen as the nonpersonalized gain of –200 (mg/dL)/(U/h) [49]–[51]. The maximum delay uncertainty tested was 30 min.

The results of the robust stability analysis are shown in Figure 8(a). The results show that the system will remain stable for large model uncertainty for both IP and SC insulin, even with a sensor time constant of 30 min, for the most aggressive tuning tested ($\tau_C = 0.1\tau_{dom}$). For the larger three values of τ_C, robust stability is maintained for all gain and delay uncertainties tested.

Increasing the sensor time constant may cause a loss of robust performance even for small model uncertainty [Figure 8(b) and (c)]. Thus, there is less tolerance for model uncertainty when the sensor time constant is increased, and it is possible that the robust performance specifications will not be met. In fact, the SC system does not meet robust performance specifications for gain uncertainties greater than 0.1 when using the most aggressive tuning tested, even for the ideal sensor case. The same analysis for $\tau_C = 0.3\tau_{dom}$ shows that the SC system is able to retain robust performance for small amounts of model uncertainty. Overall, the IP system displays a higher robust performance than the SC system. This trend is expected as a result of the faster actuation afforded by IP insulin delivery.

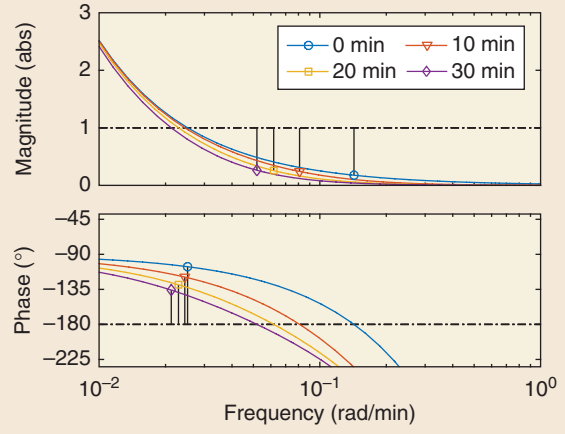

FIGURE 7 A Bode plot demonstrating the calculation of the gain and phase margin for the controller designed for intraperitoneal insulin. The plot is shown for $\tau_C = 0.1\tau_{dom}$ and for various values of τ_S. The gain margin is calculated by $1/(AR_c)$, where AR_c is the magnitude at the critical frequency where the phase crosses –180°. The phase margin is calculated as $180^\circ + \phi_g$, where ϕ_g is the phase at the gain-crossover frequency where the magnitude equals one [45].

Retaining stability in the AP system is of utmost importance, so it is encouraging to see that both the SC and the IP systems will be robustly stable even for large sensor time constants. Robust performance will be retained for low sensor time constants but may be lost if there is too much lag in the glucose measurement. For this reason, more experimental data should be collected to determine the sensor

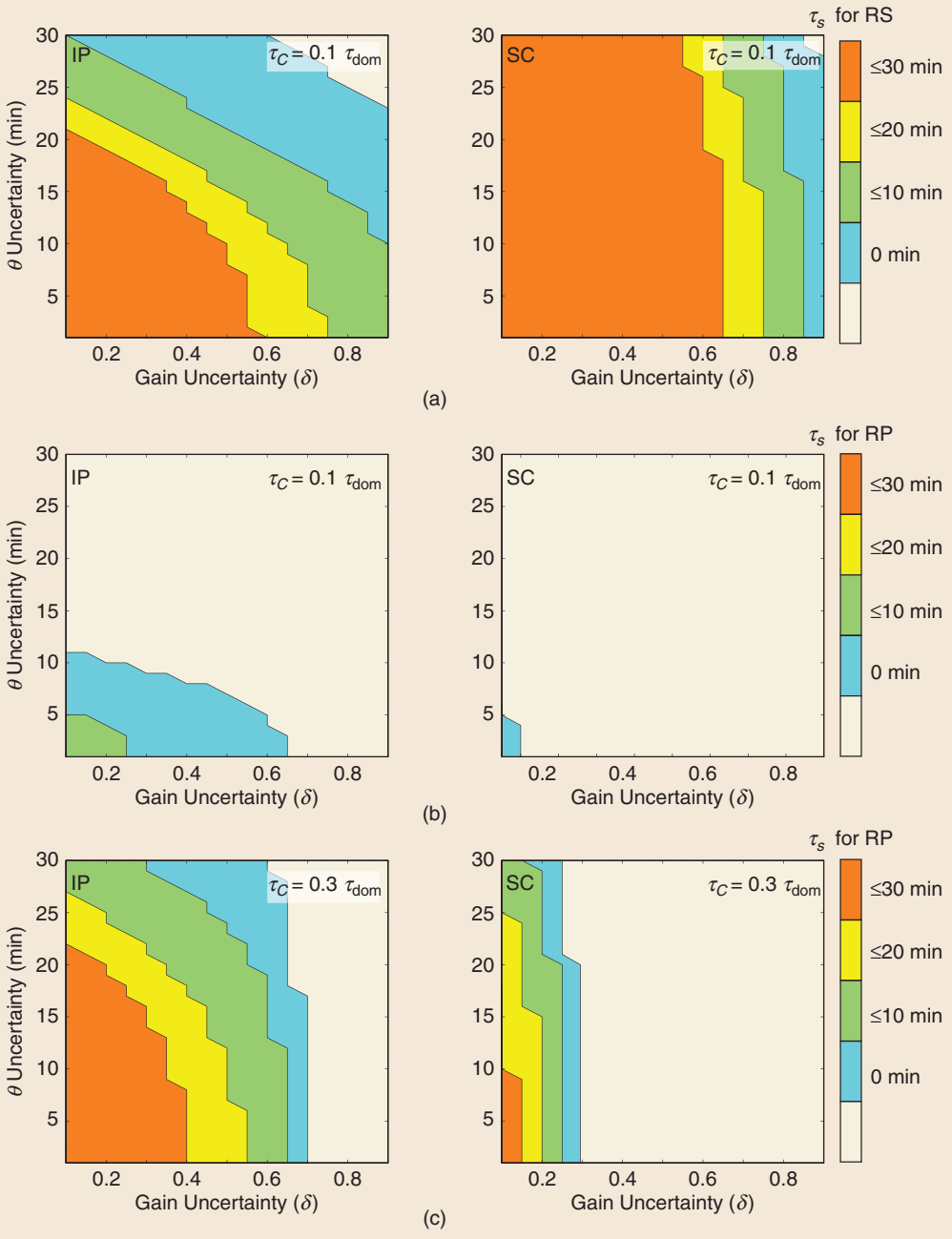

FIGURE 8 The gain and delay uncertainty allowed while still retaining (a) robust stability and [(b) and (c)] robust performance for various sensor time constants using intraperitoneal (IP) and subcutaneous (SC) insulin. Panels (a) and (b) show the analysis for a fixed τ_C of $0.1\tau_{dom}$. Robust stability was met for large amounts of model uncertainty for both systems, but the IP system performance was more robust to model uncertainty than the SC system. The analysis was repeated for a more conservative τ_C of $0.3\tau_{dom}$, for which the robust performance results are shown (c). The robust stability results for $\tau_C = 0.3\tau_{dom}$ are not shown because the system was robustly stable for all conditions tested [37].

lags present in systems being used in clinic, and new sensing methods that would provide a faster glucose measurement should be investigated. Two studies that have already been conducted to measure the lag between the intravascular and interstitial compartments of humans are presented in [56] and [57].

Simulation Studies

Simulation Methods

In silico tests were performed to evaluate the impact that sensor dynamics have on the time-domain performance of the AP. The simulations were conducted using the UVA/Padova

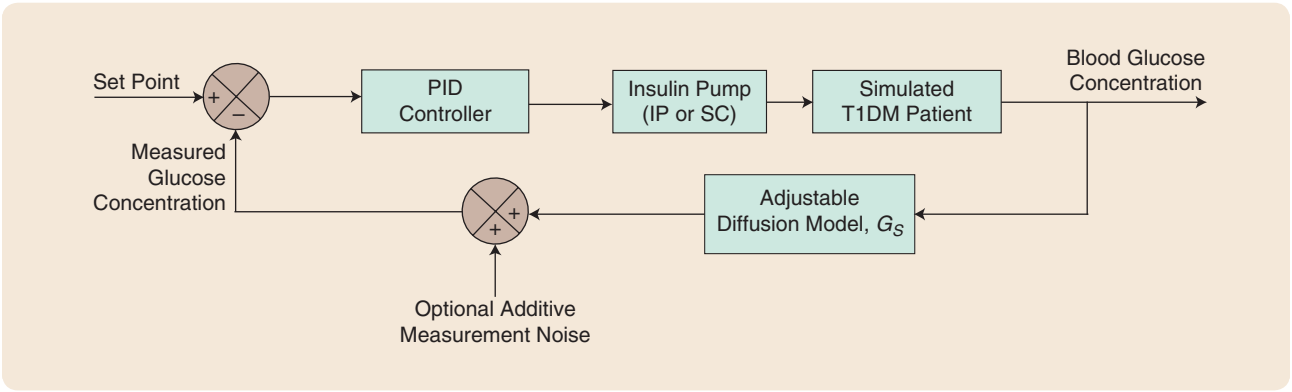

FIGURE 9 A block diagram showing the closed-loop simulation setup. The proportional-integral-derivative (PID) controller receives the error between the setpoint and the measured glucose concentration and sends an insulin dose to the simulated patient by using either the intraperitoneal (IP) or subcutaneous (SC) insulin delivery route. The resulting blood glucose concentration is passed through the glucose diffusion model with an adjustable time constant. Measurement noise can optionally be added before obtaining the measured glucose concentration [37].

metabolic simulator with ten unique simulated adult subjects with T1DM [58]. This simulator allows AP controllers to be evaluated under many different scenarios to optimize the design before moving to clinical studies. The use of the simulator also allows controlled studies to be performed that would not be possible in real life, such as testing various specified sensor time constants.

A block diagram depicting the simulation setup is shown in Figure 9. The simulator contains ports for SC and intravenous (IV) insulin delivery routes. The simulations of AP control with SC insulin delivery were conducted using the SC port. As in previous work [50], the IV port in the simulator was used as an engineering approximation of the faster insulin absorption and action that would be observed with IP insulin delivery since the characteristics of the two routes are similar [59], [60]. The insulin delivery was restricted to discrete boluses in increments of 0.05 U, to simulate the minimum stroke volume of the insulin pump.

The sensor dynamics were implemented by passing the BG through the first-order model given by (2) before sending the measurement to the controller. The sensor time constants tested, chosen to represent the range of experimental values observed in [31], were 0, 10, 20, and 30 min. The additive measurement noise was disabled to isolate the effects of the sensor dynamics on the controller performance. The reader is referred to [39] and [61] that explore glucose sensor noise and calibration errors in AP applications. The protocol tested was a fasting period followed by an unannounced meal disturbance (output disturbance) consisting of 75 g of carbohydrates (CHO).

Simulation Results and Discussion

The data from one representative subject are shown in Figure 10. When the glucose measurement is delayed, it effectively filters the controller action. The peak insulin delivery is shifted later in time, and the overall response of the AP is more sluggish. The simulation results for all ten subjects are summarized in Table 5, along with the mean and standard deviation for the time spent in hyperglycemia (BG >180 mg/dL, t_{hyper}), the area of the region below the glucose curve and above the 180 mg/dL hyperglycemia cutoff (AUC), the peak BG, and the minimum BG. For both IP and SC insulin delivery, increasing the sensor time constant significantly raised the maximum BG that was experienced, while it significantly lowered the minimum BG. This is the expected trend that would be caused by a lagging measurement.

Figure 11 shows a plot of the maximum versus minimum BG for all ten subjects, with error bars showing the standard deviation. The plot includes three representative PID choices for τ_C based on the dominant time constant for

TABLE 5 In silico performance measures for varying τ_S, with $\tau_C = 0.1\tau_{\text{dom}}$ [37]. AUC: area under the curve; BG: blood glucose. Note: *Statistically different from $\tau_s = 0$ min by paired t-test.

Intraperitoneal Delivery

τ_S (min)	t_{hyper} (min)	AUC (min · mg/dL)	Max BG (mg/dL)	Min BG (mg/dL)
0	38 ± 25	381 ± 343	192 ± 9	86 ± 5
10	50 ± 20*	761 ± 495*	202 ± 12*	83 ± 6*
20	59 ± 19*	1141 ± 670*	208 ± 14*	78 ± 7*
30	67 ± 19*	1508 ± 834*	213 ± 16*	72 ± 10*

Subcutaneous Delivery

τ_S (min)	t_{hyper} (min)	AUC (min · mg/dL)	Max BG (mg/dL)	Min BG (mg/dL)
0	107 ± 25	3643 ± 1829	231 ± 23	88 ± 5
10	113 ± 23*	4354 ± 2082*	237 ± 26*	80 ± 14
20	120 ± 22*	4957 ± 2329*	242 ± 28*	71 ± 17*
30	126 ± 22*	5510 ± 2577*	245 ± 30*	62 ± 17*

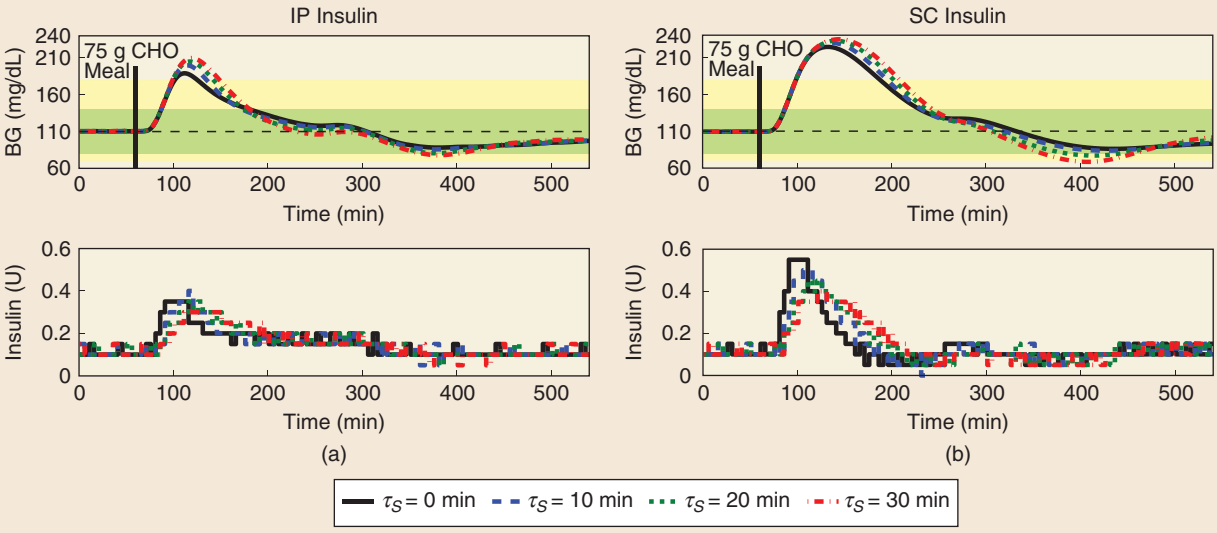

FIGURE 10 A representative result from one subject in the UVA/Padova metabolic simulator (adult subject 1) with four different values for the sensor time constant using (a) intraperitoneal (IP) insulin and (b) subcutaneous (SC) insulin. In both cases, $\tau_c = 0.1\tau_{dom}$. The plot shows the glucose concentration and insulin delivery for 1 h before and 8 h after an unannounced 75-g carbohydrates (CHO) meal disturbance. The green and yellow zones represent the tight clinical range (80–140 mg/dL) and safe clinical range (70–180 mg/dL) for the blood glucose (BG) concentration. The setpoint is shown by the horizontal dashed line at 110 mg/dL [37].

each system. On this plot, improved controller performance is indicated by proximity to the lower left corner. In all cases, decreasing the sensor time constant improved the controller performance by moving the point on the plot down and to the left. The standard deviation spread also became narrower as the sensor time constant decreased, meaning that the system is more reliable for all subjects. An increased sensor lag is detrimental to SC control because it necessitates a more conservative tuning to be used to avoid dangerous hypoglycemia (BG <70 mg/dL), at the expense of allowing more hyperglycemia.

More telling than the magnitude of the peak BG is the increased period of hyperglycemia following the meal caused by an increased sensor lag. The time spent in hyperglycemia increased by 21 ± 8 min for IP insulin and by 13 ± 3 min for SC insulin for a τ_S of 20 min as compared to the ideal sensor case. According to experimental data from [31] and [61], 20 min serves as a conservative estimate for the time constant of an SC sensor, so it would be plausible to observe this amount of lag in a clinical AP study. The cumulative time spent in hyperglycemia over a person's lifetime determines the severity of long-term health complications [2]. The increased hyperglycemia brought about by a lagging measurement will add up each time there is a meal disturbance and could result in a worse overall health outcome for the patient.

Decreasing the sensor lag had a more pronounced effect for IP insulin delivery than for SC insulin delivery, due to the significant delays in insulin action that exist in the SC system. The results for IP insulin delivery are shown in more detail in Figure 12. The box plot shows the amount of time in hyperglycemia and AUC in hyperglycemia following the meal for the ten simulated subjects using IP insulin. Both the time and the AUC in hyperglycemia increased greatly as the sensor time constant increased. For a sensor time constant as small as 10 min, the mean AUC was doubled as compared to the ideal sensor when using IP insulin delivery.

The effect of the characteristic time constant τ_C is demonstrated in Figure 13, which shows the results for the same representative subject as in Figure 10 for IP insulin using the four different values of τ_C. A larger value of τ_C leads to a slower and less aggressive response from the controller. A controller with a large value of τ_C is not able to respond in a timely manner to the rapid change in glucose caused by a meal. The same pattern is observed with increasing τ_C for the case of SC insulin (not shown). Using a smaller value of τ_C is desirable as long as the system will remain robust to model uncertainty and sensor lag.

Decreasing the sensor time constant would improve the ability of the AP to reject a meal disturbance. If such a decrease is not possible, other measures such as feedforward action may be necessary to obtain the desired level of performance. For example, the user of the AP could announce that a meal is about to be consumed, which would cue the AP to deliver a preemptive dose of insulin. While this configuration is being used more often in clinical studies [10], it is not ideal because it involves a human in the loop, which could lead to safety risks. A faster sensor could

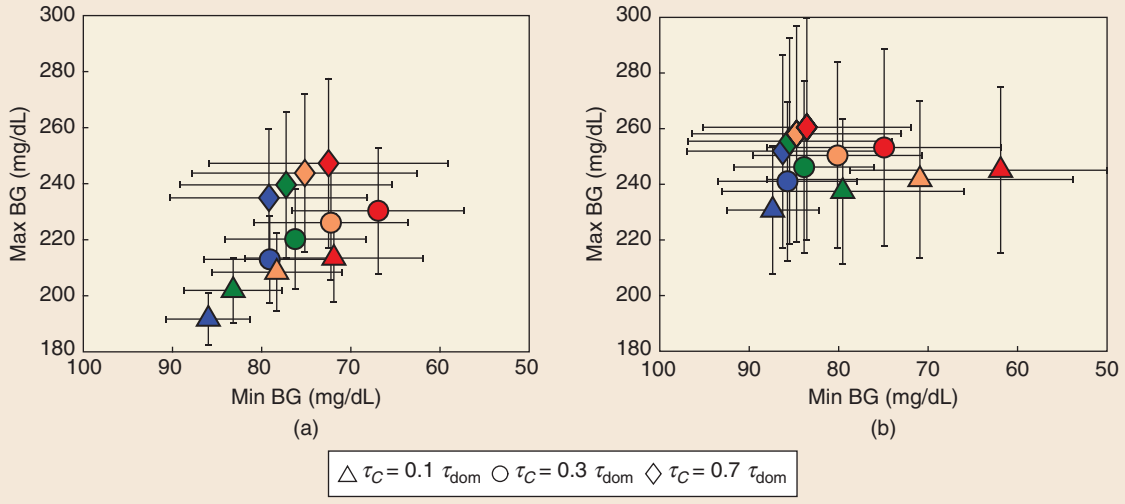

FIGURE 11 The mean maximum versus mean minimum blood glucose (BG) concentration for different sensor time constants and tuning parameters. The sensor time constants are represented by the blue (0 min), green (10 min), orange (20 min), and red (30 min) icons. The results are shown for (a) intraperitoneal insulin delivery and (b) subcutaneous insulin delivery after a 75-g carbohydrate meal disturbance. Error bars show plus or minus one standard deviation. Decreasing the sensor time constant causes the data points to move down and to the left, indicating an improvement in controller response to the meal disturbance [37].

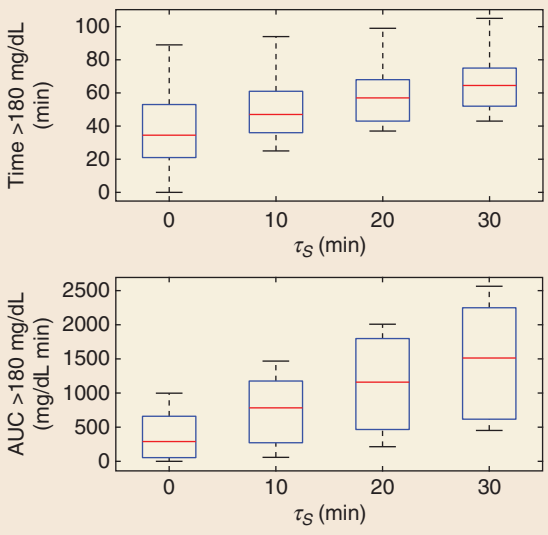

FIGURE 12 A box plot showing the amount of time spent in hyperglycemia and the area under the curve (AUC) in hyperglycemia for closed-loop control in 10 in silico subjects using intraperitoneal insulin with $\tau_C = 0.1\tau_{dom}$. The results are compared for several different values of τ_S. The red line represents the median value, the blue box represents the interquartile range, and the black bars represent the range.

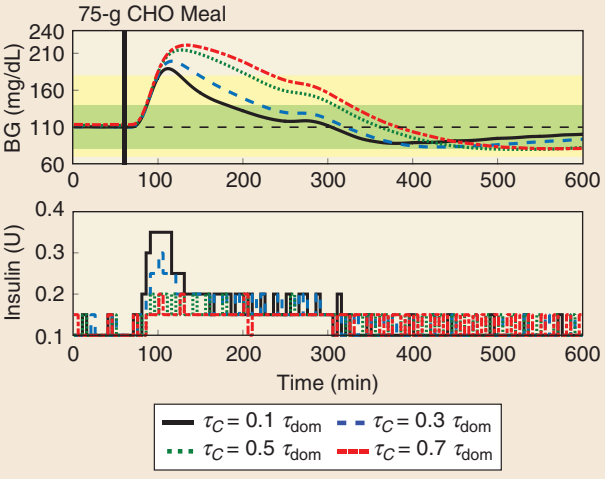

FIGURE 13 A representative result from one subject in the UVA/Padova metabolic simulator (adult subject 1) with four different values for the characteristic time constant using intraperitoneal insulin. The sensor time constant for this case was 0 min. The plot shows the glucose concentration and insulin delivery for 1 h before and 9 h after an unannounced 75-g carbohydrate (CHO) meal disturbance. The green and yellow zones represent the tight clinical range (80–140 mg/dL) and safe clinical range (70–180 mg/dL) for the blood glucose (BG) concentration. The setpoint is shown by the horizontal dashed line at 110 mg/dL.

potentially avoid the need for this feedforward action, leaving less burden on the AP user. Still, there may be a limit to the sensing speed that can be achieved. The cost of developing and manufacturing a faster sensor must be weighed against the benefit gained from the reduced lag.

CONCLUSION AND FUTURE WORK

When evaluating a new sensor technology, the pointwise error is frequently reported to demonstrate acceptable accuracy; however, a pointwise error that passes thresholds for safety could still include error from a dynamic lag that could

The relative improvement achieved by reducing sensor lag in simulation is higher when using IP insulin delivery than when using SC insulin delivery.

cause problems for an AP controller. Closed-loop simulations show that decreasing the glucose sensor lag reduces the period of hyperglycemia following a meal disturbance, which could in turn lead to a better health outcome for the patient. The relative improvement achieved by reducing sensor lag in simulation is higher when using IP insulin delivery than when using SC insulin delivery. This difference is attributable to the fact that delays present in SC insulin actuation cause the sensor lag to have less of an impact. In addition to improved glycemic control, systems with a lower sensor lag have a higher tolerance for model uncertainty resulting from inter- and intrapatient variabilities.

Glucose sensor lag is one of several factors that can affect the measurement performance. Another important factor is error in the calibration of the sensor, which can lead to a significant offset between the sensor measurement and the true BG value. This difference can have a detrimental effect on controller performance, as demonstrated in [62]. This study found that the PID controller used was not robust to calibration errors causing sensor values to be 33% higher than true BG, a level of error that may be observed with home glucose meter use. Efforts are being made to reduce calibration error with the use of a run-to-run approach [63] as well as with the development of a factory-calibrated sensor [42]. The techniques used in this article could be extended to examine other factors affecting sensor performance, such as miscalibration, to determine the level of accuracy needed for safe and effective control.

The use of an insulin delivery route with faster pharmacokinetic and pharmacodynamic characteristics (IP rather than SC) improves control performance greatly, but that improvement is only partially realized if the sensor with a large dynamic lag is used. Further experimental investigation of glucose sensor placement will reveal the extent to which the diffusion lag can be eliminated. The benefit gained from this lag reduction must be weighed against the cost and invasiveness of such a sensor to determine the best solution for the patient. The approach presented here can be used by researchers developing new sensor technologies and new AP algorithms to determine whether the tradeoff between sensor lag and clinical outcome is acceptable for their particular application.

ACKNOWLEDGMENTS

The authors acknowledge that access to the complete version of the UVA/Padova metabolic simulator was provided by an agreement with Prof. C. Cobelli (University of Padova) and Prof. B.P. Kovatchev (UVA) for research purposes. This work was supported by funding from the National Science Foundation Graduate Research Fellowship Program and the National Institutes of Health grant DP3DK101068. A preliminary version of this article was presented at the 2015 American Control Conference, Chicago, July 2015 (DOI: 10.1109/ACC.2015.7172137) [37].

AUTHOR INFORMATION

Lauren M. Huyett received the B.S. degree in chemical engineering in 2011 from Lafayette College, Easton, Pennsylvania, and the Ph.D. degree in chemical engineering from the University of California, Santa Barbara, in 2016. In 2011 she was awarded the National Science Foundation Graduate Research Fellowship. Her research interests include the translation of developments in medical device technology from the bench to the bedside.

Eyal Dassau is a senior research fellow in biomedical engineering at the Harvard John A. Paulson School of Engineering and Applied Sciences. He also holds an appointment as adjunct faculty at the Joslin Diabetes Center, Boston, Massachusetts. He received the B.Sc., M.Sc., and Ph.D. degrees in chemical engineering, in 1999, 2002, and 2006, respectively, from Technion Israel Institute of Technology, Haifa. His previous appointment was as senior investigator and diabetes research manager with the University of California, Santa Barbara. He is also an adjunct senior investigator with the William Sansum Diabetes Center, Santa Barbara. His current research interests include the modeling, design, and control of an artificial pancreas for type 1 diabetes mellitus and process and product design with an emphasis on medical and biomedical applications. He is a Senior Member of the IEEE and the American Institute of Chemical Engineering and a member of the American Diabetes Association.

Howard C. Zisser serves as an adjunct professor in chemical engineering at the University of California, Santa Barbara. He received the B.S. degree from the University of Florida, Gainesville, and the M.D. degree from The Johns Hopkins University School of Medicine, Baltimore, Maryland. His previous appointments include the director of clinical research at the William Sansum Diabetes Center, Santa Barbara, and medical director of Insulet, Billerica, Massachusetts. He is currently the diabetes clinical lead at Verily Life Sciences, Mountain View, California.

Francis J. Doyle III (frank_doyle@seas.harvard.edu) is the John A. Paulson Dean and the John A. and Elizabeth S. Armstrong Professor of Engineering and Applied Sciences at Harvard University. He received the B.S.E. degree from

Princeton University, New Jersey, in 1985, the C.P.G.S. degree from the University of Cambridge, United Kingdom, in 1986, and the Ph.D. degree from the California Institute of Technology, Pasadena, in 1991, all in chemical engineering. His previous appointment was as the Duncan and Suzanne Mellichamp Chair in process control in the Department of Chemical Engineering, University of California, Santa Barbara. He is also an adjunct senior investigator with the William Sansum Diabetes Center, Santa Barbara. His research interests include systems biology, network science, modeling and analysis of circadian rhythms, drug delivery for diabetes, model-based control, and control of particulate processes. He is a Fellow of the IEEE as well as a number of societies, including the International Federation of Automatic Control, the American Institute of Medical and Biological Engineering, and the American Association for the Advancement of Science. In 2005, he was awarded the Computing in Chemical Engineering Award from the American Institute of Chemical Engineers for his innovative research in systems biology. Additionally, he was awarded the 2015 Controls Engineering Practice Award for his pioneering work on the artificial pancreas. He can be contacted at Harvard John A. Paulson School of Engineering and Applied Sciences, 29 Oxford St., Cambridge, MA 02138 USA.

REFERENCES

[1] R. I. G. Holt, *Textbook of Diabetes*, 4th ed. Hoboken, NJ: Wiley-Blackwell, 2010.

[2] The Diabetes Control and Complications Trial Research Group, "The effect of intensive treatment of diabetes on the development and progression of long-term complications in insulin-dependent diabetes mellitus," *New Engl. J. Med.*, vol. 329, no. 14, pp. 977–986, 1993.

[3] W. Bryant, J. R. Greenfield, D. J. Chisholm, and L. V. Campbell, "Diabetes guidelines: Easier to preach than to practise?," *Med. J. Australia*, vol. 185, no. 6, pp. 305–309, 2006.

[4] K. M. Miller, N. C. Foster, R. W. Beck, R. M. Bergenstal, S. N. DuBose, L. A. DiMeglio, D. M. Maahs, and W. V. Tamborlane, "Current state of type 1 diabetes treatment in the U.S.: Updated data from the T1D exchange clinic registry," *Diabetes Care*, vol. 38, no. 6, pp. 971–978, 2015.

[5] J. R. Wood, K. M. Miller, D. M. Maahs, R. W. Beck, L. A. DiMeglio, I. M. Libman, M. Quinn, W. V. Tamborlane, and S. E. Woerner, and for the T1D Exchange Clinic Network, "Most youth with type 1 diabetes in the T1D exchange clinic registry do not meet American Diabetes Association or International Society for Pediatric and Adolescent Diabetes clinical guidelines," *Diabetes Care*, vol. 36, no. 7, pp. 2035–2037, 2013.

[6] A. M. Albisser, B. S. Leibel, T. G. Ewart, Z. Davidovac, C. K. Botz, and W. Zingg, "An artificial endocrine pancreas," *Diabetes*, vol. 23, no. 5, pp. 389–396, 1974.

[7] R. Hovorka, L. J. Chassin, M. E. Wilinska, V. Canonico, J. A. Akwi, M. O. Federici, M. Massi-Benedetti, I. Hutzli, C. Zaugg, H. Kaufmann, M. Both, T. Vering, H. C. Schaller, L. Schaupp, M. Bodenlenz, and T. R. Pieber, "Closing the loop: The adicol experience," *Diabetes Technol. Therapeut.*, vol. 6, no. 3, pp. 307–318, 2004.

[8] G. M. Steil, K. Rebrin, C. Darwin, F. Hariri, and M. F. Saad, "Feasibility of automating insulin delivery for the treatment of type 1 diabetes," *Diabetes*, vol. 55, no. 12, pp. 3344–3350, 2006.

[9] R. Voelker. "Artificial pancreas is approved," *JAMA*, vol. 316, no. 19, p. 1957, 2016. doi: 10.1001/jama.2016.16344

[10] F. J. Doyle, III, L. M. Huyett, J. B. Lee, H. C. Zisser, and E. Dassau, "Closed-loop artificial pancreas systems: Engineering the algorithms," *Diabetes Care*, vol. 37, no. 5, pp. 1191–1197, 2014.

[11] American Diabetes Association, "Standards of medical care in diabetes–2017," *Diabetes Care*, vol. 40, pp. S1–S112, Jan. 2017.

[12] D. M. Maahs, B. A. Buckingham, J. R. Castle, A. Cinar, E. R. Damiano, E. Dassau, J. H. DeVries, F. J. Doyle, S. C. Griffen, A. Haidar, L. Heinemann, R. Hovorka, T. W. Jones, C. Kollman, B. Kovatchev, B. L. Levy, R. Nimri, D. N. ONeal, M. Philip, E. Renard, S. J. Russell, S. A. Weinzimer, H. Zisser, and J. W. Lum, "Outcome measures for artificial pancreas clinical trials: A consensus report," *Diabetes Care*, vol. 39, no. 7, pp. 1175–1179, 2016.

[13] B. H. McAdams and A. A. Rizvi, "An overview of insulin pumps and glucose sensors for the generalist," *J. Clin. Med.*, vol. 5, no. 1, pp. 5, 2016.

[14] R. B. Shah, M. Patel, D. M. Maahs, and V. N. Shah, "Insulin delivery methods: Past, present and future," *Int. J. Pharmaceut. Investigat.*, vol. 6, no. 1, pp. 1–9, 2016.

[15] K. Rebrin and G. M. Steil, "Can interstitial glucose assessment replace blood glucose measurements?" *Diabetes Technol. Therapeut.*, vol. 2, no. 3, pp. 461–472, 2000.

[16] C. C. Palerm, "Physiologic insulin delivery with insulin feedback: A control systems perspective," *Comput. Methods Program Biomed.*, vol. 102, no. 2, pp. 130–137, 2011.

[17] M. Loutseiko, G. Voskanyan, D. B. Keenan, and G. M. Steil, "Closed-loop insulin delivery utilizing pole placement to compensate for delays in subcutaneous insulin delivery," *J. Diabetes Sci. Technol.*, vol. 5, no. 6, pp. 1342–1351, 2011.

[18] B. Grosman, E. Dassau, H. C. Zisser, L. Jovanovič, and F. J. Doyle, III, "Zone model predictive control: A strategy to minimize hyper- and hypoglycemic events," *J. Diabetes Sci. Technol.*, vol. 4, no. 4, pp. 961–975, 2010.

[19] A. Facchinetti, G. Sparacino, and C. Cobelli, "Enhanced accuracy of continuous glucose monitoring by online extended Kalman filtering," *Diabetes Technol. Therapeut.*, vol. 12, no. 5, pp. 353–363, 2010.

[20] B. Keenan, J. J. Mastrototaro, S. A. Weinzimer, and G. M. Steil, "Interstitial fluid glucose time-lag correction for real-time continuous glucose monitoring," *Biomed. Signal Process. Control*, vol. 8, no. 1, pp. 81–89, 2013.

[21] A. El Fathi, M. Smaoui, B. Boulet, V. Gingras, R. Rabasa-Lhoret, and A. Haidar, "The artificial pancreas and meal control," *IEEE Control Syst. Mag.*, vol. 38, no. 1, pp. 67–85, 2017.

[22] B. Grosman, J. Ilany, A. Roy, N. Kurtz, D. Wu, N. Parikh, G. Voskanyan, N. Konvalina, C. Mylonas, R. Gottlieb, F. Kaufman, and O. Cohen, "Hybrid closed-loop insulin delivery in type 1 diabetes during supervised outpatient conditions," *J. Diabetes Sci. Technol.*, vol. 10, no. 3, pp. 708–713, 2016.

[23] S. J. Russell, M. A. Hillard, C. Balliro, K. L. Magyar, R. Selagamsetty, M. Sinha, K. Grennan, D. Mondesir, L. Ehklaspour, H. Zheng, E. R. Damiano, and F. H. El-Khatib, "Day and night glycaemic control with a bionic pancreas versus conventional insulin pump therapy in preadolescent children with type 1 diabetes: A randomised crossover trial," *Lancet Diabetes Endocrinol.*, vol. 4, no. 3, pp. 233–243, 2016.

[24] T. T. Ly, A. Roy, B. Grosman, J. Shin, A. Campbell, S. Monirabbasi, B. Liang, R. v. Eyben, S. Shanmugham, P. Clinton, and B. A. Buckingham, "Day and night closed-loop control using the integrated Medtronic hybrid closed-loop system in type 1 diabetes at diabetes camp," *Diabetes Care*, vol. 38, no. 7, pp. 1205–1211, 2015.

[25] H. Thabit, M. Tauschmann, J. M. Allen, L. Leelarathna, S. Hartnell, M. E. Wilinska, C. L. Acerini, S. Dellweg, C. Benesch, L. Heinemann, J. K. Mader, M. Holzer, H. Kojzar, J. Exall, J. Yong, J. Pichierri, K. D. Barnard, C. Kollman, P. Cheng, P. C. Hindmarsh, F. M. Campbell, S. Arnolds, T. R. Pieber, M. L. Evans, D. B. Dunger, and R. Hovorka, "Home use of an artificial beta cell in type 1 diabetes," *New Engl. J. Med.*, vol. 373, no. 22, pp. 2129–2140, 2015.

[26] M. Tauschmann, J. M. Allen, M. E. Wilinska, H. Thabit, Z. Stewart, P. Cheng, C. Kollman, C. L. Acerini, D. B. Dunger, and R. Hovorka, "Day-and-night hybrid closed-loop insulin delivery in adolescents with type 1 diabetes: A free-living, randomized clinical trial," *Diabetes Care*, vol. 39, no. 7, pp. 1168–1174, 2016.

[27] E. Dassau, S. A. Brown, A. Basu, J. E. Pinsker, Y. C. Kudva, R. Gondhalekar, S. Patek, D. Lv, M. Schiavon, J. B. Lee, C. Dalla Man, L. Hinshaw, K. Castorino, A. Mallad, V. Dadlani, S. K. McCrady-Spitzer, M. McElwee-Malloy, C. A. Wakeman, W. C. Bevier, P. K. Bradley, B. Kovatchev, C. Cobelli, H. C. Zisser, and F. J. Doyle, III, "Adjustment of open-loop settings to improve closed-loop results in type 1 diabetes: A multicenter randomized trial," *J. Clin. Endocrinol. Metab.*, vol. 100, no. 10, pp. 3878–3886, 2015.

[28] A. Liebl, R. Hoogma, E. Renard, P. H. L. M. Geelhoed-Duijvestijn, E. Klein, J. Diglas, L. Kessler, V. Melki, P. Diem, J.-M. Brun, P. Schaepelynck-Blicar, and T. Frei, and for the European DiaPort Study Group, "A reduction in severe hypoglycaemia in type 1 diabetes in a randomized crossover study of continuous intraperitoneal compared with subcutaneous insulin infusion," *Diabetes Obesity Metabol.*, vol. 11, no. 11, pp. 1001–1008, 2009.

[29] D. M. Nathan, F. L. Dunn, J. Bruch, C. McKitrick, M. Larkin, C. Haggan, J. Lavin-Tompkins, D. Norman, D. Rogers, and D. Simon, "Postprandial insulin profiles with implantable pump therapy may explain decreased frequency of severe hypoglycemia, compared with intensive subcutaneous regimens, in insulin-dependent diabetes mellitus patients," *Am. J. Med.*, vol. 100, no. 4, pp. 412–417, 1996.
[30] N. Spaan, A. Teplova, G. Stam, J. Spaan, and C. Lucas, "Systematic review: Continuous intraperitoneal insulin infusion with implantable insulin pumps for diabetes mellitus," *Acta Diabetol.*, vol. 51, no. 3, pp. 339–351, 2014.
[31] D. R. Burnett, L. M. Huyett, H. C. Zisser, F. J. Doyle, III, and B. D. Mensh, "Glucose sensing in the peritoneal space offers faster kinetics than sensing in the subcutaneous space," *Diabetes*, vol. 63, no. 7, pp. 2498–2505, 2014.
[32] P. van Dijk, S. Logtenberg, R. Gans, H. Bilo, and N. Kleefstra, "Intraperitoneal insulin infusion: Treatment option for type 1 diabetes resulting in beneficial endocrine effects beyond glycaemia," *Clin. Endocrinol.*, vol. 81, no. 4, pp. 488–497, 2014.
[33] J. J. Lee, E. Dassau, H. Zisser, W. Tamborlane, S. Weinzimer, and F. J. Doyle, III, "The impact of insulin pharmacokinetics and pharmacodynamics on the closed-loop artificial pancreas," in *Proc. 52nd IEEE Conf. Decision and Control*, 2013, pp. 127–132.
[34] H. Zisser, E. Dassau, J. J. Lee, R. A. Harvey, W. Bevier, and F. J. Doyle, III, "Clinical results of an automated artificial pancreas using technosphere inhaled insulin to mimic first-phase insulin secretion," *J. Diabetes Sci. Technol.*, vol. 9, no. 3, pp. 564–572, 2015.
[35] E. Renard, J. Place, M. Cantwell, H. Chevassus, and C. C. Palerm, "Closed-loop insulin delivery using a subcutaneous glucose sensor and intraperitoneal insulin delivery: Feasibility study testing a new model for the artificial pancreas," *Diabetes Care*, vol. 33, no. 1, pp. 121–127, 2010.
[36] J. J. Lee, E. Dassau, H. Zisser, R. A. Harvey, L. Jovanovič, and F. J. Doyle, III, "In silico evaluation of an artificial pancreas combining exogenous ultrafast-acting technosphere insulin with zone model predictive control," *J. Diabetes Sci. Technol.*, vol. 7, no. 1, pp. 215–226, 2013.
[37] L. M. Huyett, E. Dassau, H. C. Zisser, and F. J. Doyle III, "The impact of glucose sensing dynamics on the closed-loop artificial pancreas," in *Proc. American Control Conf.*, 2015, pp. 5116–5121.
[38] D. B. Keenan, J. J. Mastrototaro, G. Voskanyan, and G. M. Steil, "Delays in minimally invasive continuous glucose monitoring devices: A review of current technology," *J. Diabetes Sci. Technol.*, vol. 3, no. 5, pp. 1207–1214, 2009.
[39] A. Facchinetti, S. Del Favero, G. Sparacino, J. R. Castle, W. K. Ward, and C. Cobelli, "Modeling the glucose sensor error," *IEEE Trans. Biomed. Eng.*, vol. 61, no. 3, pp. 620–629, 2014.
[40] M. Schiavon, C. Dalla Man, S. Dube, M. Slama, Y. C. Kudva, T. Peyser, A. Basu, R. Basu, and C. Cobelli, "Modeling plasma-to-interstitium glucose kinetics from multitracer plasma and microdialysis data," *Diabetes Technol. Therapeut.*, vol. 17, no. 11, pp. 825–831, 2015.
[41] A. Dehennis, M. A. Mortellaro, and S. Ioacara, "Multisite study of an implanted continuous glucose sensor over 90 days in patients with diabetes mellitus," *J. Diabetes Sci. Technol.*, vol. 9, no. 5, pp. 951–956, 2015.
[42] T. Bailey, B. W. Bode, M. P. Christiansen, L. J. Klaff, and S. Alva, "The performance and usability of a factory-calibrated flash glucose monitoring system," *Diabetes Technol. Therapeut.*, vol. 17, no. 11, pp. 787–794, 2015.
[43] R. Gifford, "Continuous glucose monitoring: 40 years, what we've learned and what's next," *Chem. Phys. Chem.*, vol. 14, no. 10, pp. 2032–2044, 2013.
[44] F. J. Ascaso and V. Huerva, "Noninvasive continuous monitoring of tear glucose using glucose-sensing contact lenses," *Optometry Vis. Sci.*, vol. 93, no. 4, pp. 426–434, 2016.
[45] D. E. Seborg, D. A. Mellichamp, T. F. Edgar, and F. J. Doyle, III, *Process Dynamics and Control*, 3rd ed. Hoboken, NJ: Wiley, 2011.
[46] R. A. Harvey, E. Dassau, H. Zisser, D. E. Seborg, L. Jovanovič, and F. J. Doyle, III, "Design of the health monitoring system for the artificial pancreas: Low glucose prediction module," *J. Diabetes Sci. Technol.*, vol. 6, no. 6, pp. 1345–1354, 2012.
[47] T. C. Dunn, R. C. Eastman, and J. A. Tamada, "Rates of glucose change measured by blood glucose meter and the glucowatch biographer during day, night, and around mealtimes," *Diabetes Care*, vol. 27, no. 9, pp. 2161–2165, 2004.
[48] R. A. Harvey, E. Dassau, W. C. Bevier, D. E. Seborg, L. Jovanovič, F. J. Doyle, III, and H. C. Zisser, "Clinical evaluation of an automated artificial pancreas using zone-model predictive control and health monitoring system," *Diabetes Technol. Therapeut.*, vol. 16, no. 6, pp. 348–357, 2014.
[49] K. van Heusden, E. Dassau, H. C. Zisser, D. E. Seborg, and F. J. Doyle, III, "Control-relevant models for glucose control using a priori patient characteristics," *IEEE Trans. Biomed. Eng.*, vol. 59, no. 7, pp. 1839–1849, 2012.
[50] J. J. Lee, E. Dassau, H. Zisser, and F. J. Doyle, III, "Design and in silico evaluation of an intraperitoneal-subcutaneous (IP-SC) artificial pancreas," *Comput. Chem. Eng.*, vol. 70, pp. 180–188, Nov. 2014.
[51] A. Tagliavini, "Development and evaluation of PID controllers for glucose control in people with type 1 diabetes mellitus," M.S. thesis, Dept. Information Engineering, Univ. Padova, Italy, 2012.
[52] G. F. Franklin, J. D. Powell, and M. L. Workman, *Digital Control of Dynamic Systems*, 3rd ed. Menlo Park, CA: Addison-Wesley, 1997.
[53] S. Skogestad, "Simple analytic rules for model reduction and PID controller tuning," *Modeling Identification Control*, vol. 25, no. 2, pp. 85–120, 2004.
[54] G. Boden, X. Chen, and J. L. Urbain, "Evidence for a circadian rhythm of insulin sensitivity in patients with NIDDM caused by cyclic changes in hepatic glucose production," *Diabetes*, vol. 45, no. 8, pp. 1044–1050, 1996.
[55] S. Skogestad and I. Postlethwaite, *Multivariable Feedback Control: Analysis and Design*, 2nd ed. Hoboken, NJ: Wiley-Interscience, 2005.
[56] A. Basu, S. Dube, M. Slama, I. Errazuriz, J. C. Amezcua, Y. C. Kudva, T. Peyser, R. E. Carter, C. Cobelli, and R. Basu, "Time lag of glucose from intravascular to interstitial compartment in humans," *Diabetes*, vol. 62, no. 12, pp. 4083–4087, 2013.
[57] A. Basu, S. Dube, S. Veettil, M. Slama, Y. C. Kudva, T. Peyser, R. E. Carter, C. Cobelli, and R. Basu, "Time lag of glucose from intravascular to interstitial compartment in type 1 diabetes," *J. Diabetes Sci. Technol.*, vol. 9, no. 1, pp. 63–68, 2015.
[58] B. P. Kovatchev, M. Breton, C. D. Man, and C. Cobelli, "In silico preclinical trials: A proof of concept in closed-loop control of type 1 diabetes," *J. Diabetes Sci. Technol.*, vol. 3, no. 1, pp. 44–55, 2009.
[59] E. Renard, "Insulin delivery route for the artificial pancreas: Subcutaneous, intraperitoneal, or intravenous? Pros and cons," *J. Diabetes Sci. Technol.*, vol. 2, no. 4, pp. 735–738, 2008.
[60] C. K. Botz, B. S. Leibel, W. Zingg, R. E. Gander, and A. M. Albisser, "Comparison of peripheral and portal routes of insulin infusion by a computer-controlled insulin infusion system (artificial endocrine pancreas)," *Diabetes*, vol. 25, no. 8, pp. 691–700, 1976.
[61] A. Facchinetti, S. Del Favero, G. Sparacino, and C. Cobelli, "Model of glucose sensor error components: Identification and assessment for new Dexcom G4 generation devices," *Med. Biol. Eng. Comput.*, vol. 53, no. 12, pp. 1259–1269, 2015.
[62] H. Wolpert, M. Kavanagh, A. Atakov-Castillo, and G. M. Steil, "The artificial pancreas: Evaluating risk of hypoglycaemia following errors that can be expected with prolonged at-home use," *Diabetic Med.*, vol. 33, no. 2, pp. 235–242, 2016.
[63] J. B. Lee, E. Dassau, and F. J. Doyle, "A run-to-run approach to enhance continuous glucose monitor accuracy based on continuous wear," in *Proc. 9th IFAC Symp. Biological and Medical Systems*, 2015, vol. 48, no. 20, pp. 237–242.
[64] D. D. Cunningham and J. A. Stenken, "In vivo glucose sensing," in *Chemical Analysis Series*. Hoboken, NJ: Wiley, 2010.
[65] K. Rebrin, G. M. Steil, W. P. van Antwerp, and J. J. Mastrototaro, "Subcutaneous glucose predicts plasma glucose independent of insulin: implications for continuous monitoring," *Am. J. Physiol. Endocrinol. Metab.*, vol. 277, no. 3, pp. E561–E571. 1999.
[66] J. R. Castle and P. G. Jacobs, "Nonadjunctive use of continuous glucose monitoring for diabetes treatment decisions," *J. Diabetes Sci. Technol.*, vol. 10, no. 5, pp. 1169–1173, 2016.
[67] H. Thabit, L. Leelarathna, M. E. Wilinska, D. Elleri, J. M. Allen, A. Lubina-Solomon, E. Walkinshaw, M. Stadler, P. Choudhary, J. K. Mader, S. Dellweg, C. Benesch, T. R. Pieber, S. Arnolds, S. R. Heller, S. A. Amiel, D. Dunger, M. L. Evans, and R. Hovorka, "Accuracy of continuous glucose monitoring during three closed-loop home studies under free-living conditions," *Diabetes Technol. Therapeut.*, vol. 17, no. 11, pp. 801–807, 2015.
[68] E. R. Damiano, K. McKeon, F. H. El-Khatib, H. Zheng, D. M. Nathan, and S. J. Russell, "A comparative effectiveness analysis of three continuous glucose monitors: The Navigator, G4 Platinum, and Enlite," *J. Diabetes Sci. Technol.*, vol. 8, no. 4, pp. 699–708, 2014.
[69] W. L. Clarke, D. Cox, L. A. Gonder-Frederick, W. Carter, and S. L. Pohl, "Evaluating clinical accuracy of systems for self-monitoring of blood glucose," *Diabetes Care*, vol. 10, no. 5, pp. 622–628, 1987.